ELSEVIER

Journal of Magnetism and Magnetic Materials 249 (2002) 251–256

journal of magnetism and magnetic materials

www.elsevier.com/locate/jmmm

Computational micromagnetism of magnetization processes in nickel nanowires

Riccardo Hertel*

Max-Planck– Institute of Microstructure Physics, Weinberg 2, 06120 Halle, Germany

Abstract

Ordered sets of interacting ferromagnetic nanowires are complex systems which require numerical simulations for the investigation of their micromagnetic properties. Applying finite element techniques combined with the boundary element method allows to accurately calculate the magnetostatic interaction between several wires. It turns out that for an array of wires the coercive field is significantly lower than it is for a single nanowire. Time-resolved micromagnetic simulations are employed to study the dynamics of the magnetization reversal of single nanowires. With increasing diameter, a nucleation–propagation process is replaced by a curling reversal mode.

PACS: 75.75.+a; 75.40.Mg; 75.60.−d; 41.20.Gz

Keywords: Computational micromagnetism; Finite element method; Magnetic nanowires; Magnetization dynamics

1. Introduction

Arrays of magnetic nanowires are interesting candidates for ultra-high-density recording media [1,2]. The small lateral expansion of about 20−50 nm in principle allows for information storage densities in the order of a few hundred Gbit/in^2. As a result from progress in the fabrication of highly ordered arrays of magnetic wires [3] and their prospective application as storage media, the micromagnetic properties of an ensemble of magnetic nanowires, and especially the understanding of their hysteretic behavior recently has become of growing interest.

The characteristic parameters of the hysteresis loop of arrays of nanowires, i.e. the coercive field and the remanence as well as the shape of the hysteresis loop, depend on the particle shape, the parameters of the magnetic material, the microstructure and on the magnetostatic interaction with the neighboring wires. The latter point is a central issue of this paper. Numerical methods are required to treat an array of interacting wires in the framework of micromagnetism.

Generally, two different approaches can be found in the literature concerning the simulation of the properties of magnetic nanowires. One way consists in modelling a large set of nanowires, which may be even infinitely extended [4,5]. Due to the complexity of the system [6], in this case it is necessary to make simplifying assumptions concerning the magnetic structure and the

*Tel.: +49-345-5582-592; fax: +49-345-5511223.
E-mail address: hertel@mpi-halle.mpg.de (R. Hertel).

0304-8853/02/$ - see front matter
PII: S0304-8853(02)00539-5

magnetostatic fields. Another strategy consists in simulating the magnetization processes in single, isolated nanowires [7–9]. Such calculations are performed from first principles in the framework of micromagnetism, i.e. without making simplifying assumptions concerning the magnetic structure of the wires and the magnetostatic fields. The drawback of this method is that a full micromagnetic simulation of a single nanowires is already involved, so that the simulation of an array of reasonable size is precluded due to the high computational costs.

In Section 4.1, micromagnetic simulations on arrays consisting of several nickel nanowires are presented. Using a boundary element method [10] it is possible to calculate the magnetostatic interaction between magnetic particles with high accuracy and without the need to consider the area between the particles [11]. The dynamics of the magnetization reversal mechanism is discussed in Section 4.2.

Two different methods are employed for micromagnetic simulations. To calculate the hysteretic properties of magnetostatically coupled nanowires a quasi-static algorithm based on energy minimization is used. The dynamics of the magnetization reversal in single nanowires, instead, is investigated by means of an algorithm which integrates Gilbert's equation of motion for the magnetic moments.

2. Micromagnetic background

Equilibrium structures of the magnetization are characterized by local minima of the Gibbs free energy. Therefore, it is possible to calculate magnetic structures by minimizing the free energy as a function of the directional field of the polarization $\boldsymbol{J}(\boldsymbol{r})$. The most important energy contributions are the exchange energy E_{exc}, the anisotropy energy E_{an}, the stray field energy E_{s} and the Zeeman energy E_{Zee} in an external field. Each of these energies results from the integration of the corresponding energy denities e over the sample's volume V

$$G = \int e \,\mathrm{d}V = \int e_{\mathrm{exc}} + e_{\mathrm{an}} + e_{\mathrm{s}} + e_{\mathrm{Zee}} \,\mathrm{d}V. \qquad (1)$$

For a given ferromagnetic material, the total energy (1) is given uniquely by the magnetization field within the sample. Numerically, this field is represented in a discretized form. The sample is subdivided into finite elements of irregular tetrahedral shape. The magnetization is calculated at the nodes of the finite element mesh. Since the magnitude of the magnetization vector is constant (saturation polarization $J_{\mathrm{s}} = |\boldsymbol{J}|$), two polar angles ($\vartheta_i$, φ_i, the angles enclosed with the z-axis and with the x-axis in the xy-plane, respectively) are sufficient to describe the direction of the magnetization at each node i. The total energy (1) can then be minimized with respect to the variables $\{\varphi_i,\vartheta_i\}$, e.g. by means of the conjugate gradient method, yielding a discretized solution of an equilibrium structure of the magnetization. Details on this procedure are described elsewhere [12].

The demagnetizing field is calculated with a magnetic scalar potential U, which is assigned to each node of the mesh and from which the demagnetizing field $\boldsymbol{H}_{\mathrm{d}} = -\boldsymbol{\nabla}U$ is derived. The magnetic scalar potential is calculated by means of a hybrid boundary element/finite element method [13]. This procedure consists essentially of splitting the potential U in two parts $U = U_1 + U_2$, of which U_1 satisfies Poisson's equation $\Delta U_1 = \boldsymbol{\nabla}\cdot\boldsymbol{J}/\mu_0$ and U_2 is the solution of Laplace's equation $\Delta U_2 = 0$ with appropriate boundary conditions. The boundary element method is employed to determine the Dirichlet boundary conditions for U_2.

The above procedure to minimize the total energy allows to calculate equilibrium structures of the magnetization. The analysis of dynamic aspects of the magnetization, however, requires a different approach. The temporal evolution of the polarization $\boldsymbol{J}$ is given by Gilbert's equation

$$\frac{\mathrm{d}\boldsymbol{J}}{\mathrm{d}t} = -\gamma(\boldsymbol{J}\times\boldsymbol{H}_{\mathrm{eff}}) + \frac{\alpha}{J_{\mathrm{s}}}\left(\boldsymbol{J}\times\frac{\mathrm{d}\boldsymbol{J}}{\mathrm{d}t}\right), \qquad (2)$$

where γ is the gyromagnetic ratio and α is a damping constant. The effective field $\boldsymbol{H}_{\mathrm{eff}}$ follows from the energy density e as the negative variational derivative with respect to the polarization $\boldsymbol{H}_{\mathrm{eff}} = -\delta e/\delta\boldsymbol{J}$.

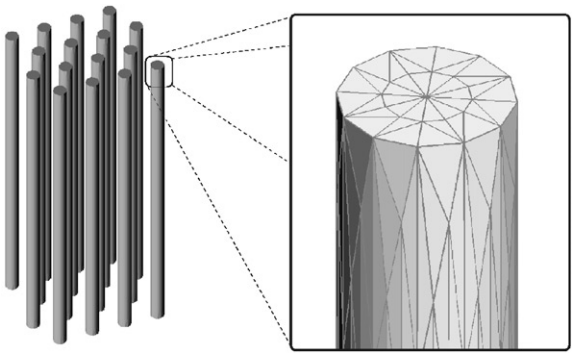

Fig. 1. Array of 16 nanowires as used for the simulation (left) and enlarged view on the top of one wire (right) illustrating the finite element discretization.

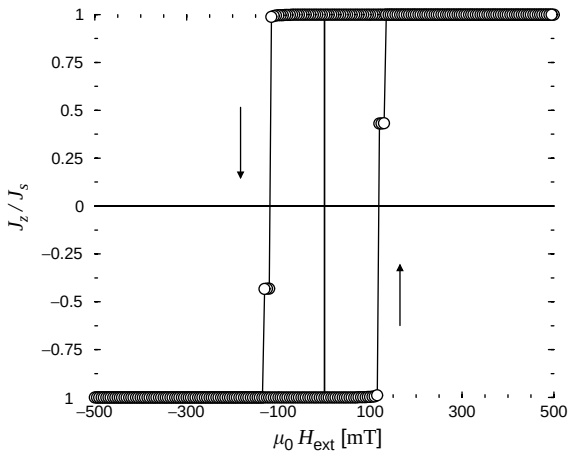

Fig. 2. Hysteresis loop of an array of seven nanowires.

3. Sample specification

Hexagonal arrays of nickel nanowires are modelled. The diameter of the wires is 40 nm and the length is 1 μm. The material's parameters are $A = 1.05 \times 10^{-11}$ J/m (exchange constant) and $J_s = 0.525$ T. The magnetocrystalline anisotropy is set to zero, since the wires are assumed to be mostly amorphous. The wires are placed on hexagonal lattice sites with a pitch of 100 nm. This data has been chosen in accordance with corresponding experimental investigations on highly ordered Nickel nanowires embedded in a porous alumina matrix [2]. The largest set considered in the present simulations is diplayed in Fig. 1.

4. Results

4.1. Hysteresis loops

To systematically investigate the effect of the magnetostatic interaction between the wires, simulations of the hysteresis loops are performed for different numbers of wires, with a maximum of 16 interacting nanowires.

The external field is applied in direction of the wires' axis. Closed hysteresis loops are simulated for values of the external fields between $+500$ and -500 mT. The field is reduced and incremented in steps of 5 mT. At each step, the magnetic structure of each wire of the considered array is calculated. Since the magnetocrystalline anisotropy is set to zero, magnetostatic effects are the only source of hysteresis. Therefore, the stray field needs to be calculated with particularly high precision.

It turns out that after saturation, each wire can be regarded as a magnetically bistable system. The nanowires switch between two well defined, mostly homogeneous magnetization states. This behavior results in a hysteresis loop of nearly rectangular shape for a single nanowire.

An example of a hysteresis loop of interacting nanowires is shown in Fig. 2 for the case of a set of seven nanowires. Configurations with reduced net magnetization can be found in the vicinity of the coercive field. This occurs when not all of the wires are magnetized in the same direction. In this case, five of the seven nanowires have switched at ± 120 mT, while two wires are still magnetized in the opposite direction.

The magnetostatic coupling between the wires strongly influences the coercive field H_C of the set of coupled wires. A monotonous reduction of H_C is found with increasing number of interacting nanowires, see Fig. 3.

While a single nanowire reverses at an opposite field of 145 mT, the coercive field is only 115 mT for an array of 16 nanowires. This significant reduction of roughly 30% is a remarkable result of the simulation which demonstrates the strong influence of the magnetostatic interaction on the

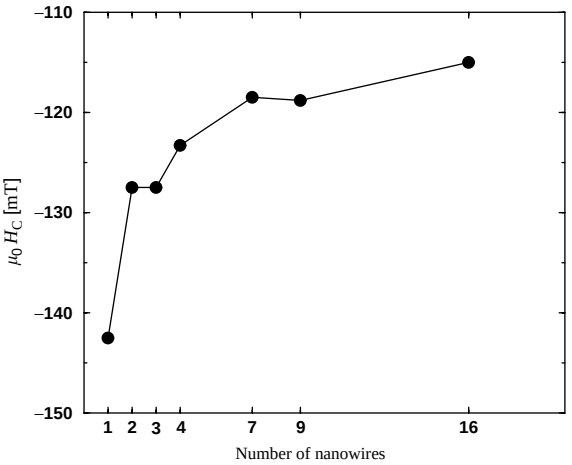

Fig. 3. The coercive field diminishes with increasing number of interacting nanowires.

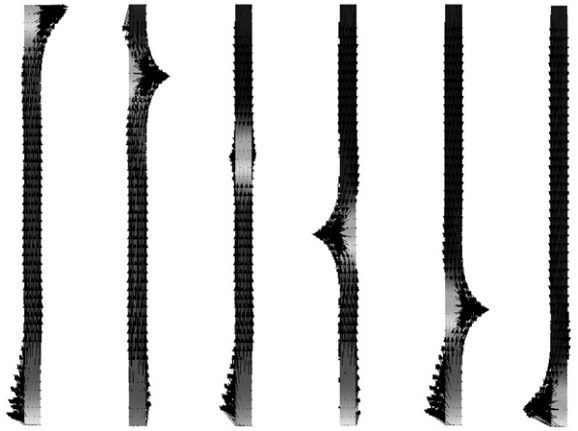

Fig. 4. Six snapshots of the reversal mechanism by means of nucleation and propagation in a nanowire of 40 nm diameter. The figures are ordered at equal steps in time, increasing from left to right.

hysteresis loop. Though the available data is not sufficient to reliably extrapolate the values of H_C to the case of an infinite number of nanowires, the tendency is obvious and a coercive field in the order of 100 mT can be expected for large numbers of nanowires. The experimentally determined value for the coercivity is 110 mT [2], which is quite close to the computed result for 16 nanowires.

4.2. Switching dynamics

The magnetization reversal is studied by means of dynamic micromagnetic simualtions. Since the reversal mechanism is unlikely to depend on the neighboring wires and the numerical effort for dynamic simulations is much higher than for quasi-static ones, the dynamic simulation is restricted to a single, isolated nanowire. An external field of sufficient strength for reversal (in this case 150 mT) is applied instantaneously to the homogeneously magnetized wire. With these initial conditions, Gilbert's equation (2) is integrated numerically at each node. A damping parameter $\alpha = 0.1$ is assumed.

It is found that the reversal mechanism depends sensitively on the diameter d of the nanowires. For $d = 40$ nm, the reversal occurs by means of nucleation and subsequent soliton propagation. Snapshots of the magnetization reversal are shown in Fig. 4. The reversal sets in at the end of the wire. There, the demagnetizing field has its strongest value and hence facilitates the reversal. The strong effect of shape anisotropy aligns the magnetization in direction of the wire axis as far as possible. This leads to the formation of a domain with reversed magnetization which expands by means of domain wall displacement. Once the reversal has started at the end of the wire, a head-on domain wall propagates through the wire. This domain wall separates two regions of different magnetization direction, one of which is oriented parallel to the external field, the other anti-parallel to it.

The magnetization in the middle of the domain wall is oriented perpendicular to the external field. This gives rise to a precession of the magnetization within the domain wall. Therefore, the soliton does not simply propagate through the wire, but it winds down the wire leading to highly regular, periodic oscillations of the magnetization components perpendicular to the wire axis, as can be seen in Fig. 5.

The magnetization reversal mechanism changes drastically if the diameter of the nanowire is larger. Snapshots of the beginning of the magnetization reversal in a nanowire with 60 nm diameter are shown in Fig. 6. Except for the larger diameter, the nanowire is the same as before.

Regarding the onset of magnetization reversal at the particle's end and the expansion of a reversed domain, this mode is similar to the previous case. However, the cross-section is now large enough to sustain a vortex, which is formed during reversal in order to reduce magnetic surface charges. The vortex formation is similar to a curling mode which in this case, however, is localized in contrast to the classical version. This process represents a mixed form of a curling reversal mode and a nucleation–propagation process. The junction between two mutually antiparallel domains is in this case a vortex wall. This mechanism is similar to a nucleation process discussed analytically by Braun [14]. Note that in the middle of the vortex a micromagnetic singularity (Bloch point) is formed which propagates through the wire. Details on this reversal mechanism will be subject of future investigations.

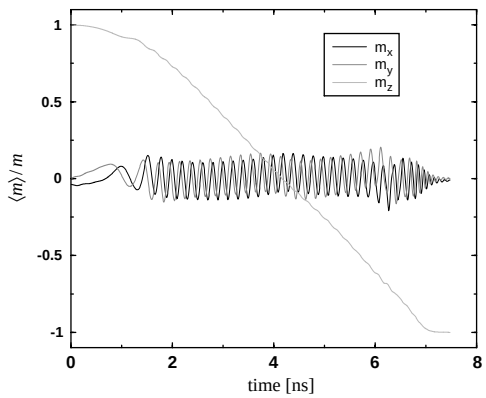

Fig. 5. Average magnetization components during the magnetization reversal. The magnetization in the xy-plane perpendicular to the wire axis oscillates with high frequency while the mean z-component decreases.

5. Conclusions

Static and dynamic micromagnetic simulations based on the finite element method combined with the boundary element method allow for detailed predictions of the micromagnetic properties of soft magnetic nanowires.

The simulations clearly show that magnetostatic coupling is crucial for the coercive field of an array of magnetic nanowires. While the calculated value of the coercive field of a single nanowire is merely of the same order of magnitude as the experimental value for the array, the simulation of a set of 16 nanowires yields a coercive field which is in close agreement with to the experimental value. However, the maximum size of the simulated array is not sufficient to expect an exact reproduction of the experimental value.

Dynamic micromagnetic simulations reveal that magnetization reversal of nickel nanowires occurs by nucleation and subsequent propagation. In thin wires ($d = 40$ nm), head-on domain walls are generated at the wire's ends which propagate

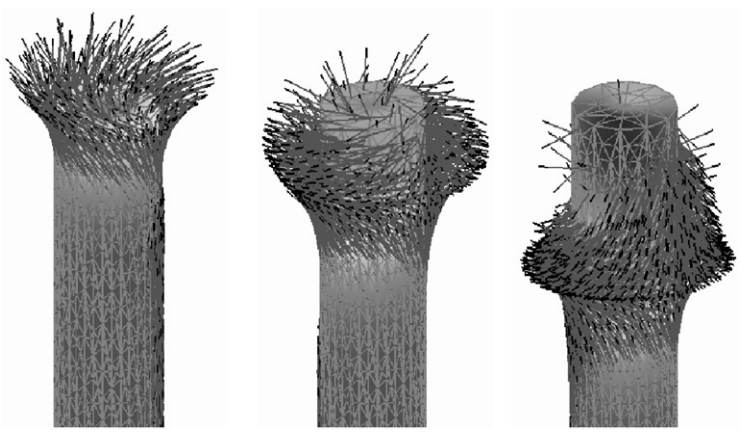

Fig. 6. Dynamics of a curling reversal mode combined with a nucleation-propagation process in a nanowire with 60 nm diameter. Snapshots are taken at increasing time from left to right.

through the wire. A characteristic oscillation of the perpendicular component is forecasted for this case. A more involved, but similar, reversal mode is found in wires of 60 nm diameter. This mixed form of a curling reversal and a nucleation–propagation process contains a head-on domain wall with vortex structure which propagates through the wire, thus reversing the magnetization in the wire.

Acknowledgements

The author is indebted to K. Nielsch, R. Wehrspohn and J. Kirschner for valuable discussions.

References

[1] C. Ross, R. Chantrell, M. Hwang, M. Farhoud, T. Savas, Y. Hao, H. Smith, F. Ross, M. Redjdal, F. Himphrey, Phys. Rev. B 62 (2000) 14252.
[2] K. Nielsch, R.B. Wehrspohn, J. Barthel, J. Kirschner, U. Gösele, S.F. Fischer, H. Kronmüller, Appl. Phys. Lett. 79 (2001) 1360.
[3] K. Nielsch, F. Müller, A. Li, U. Gösele, Adv. Mater. 12 (2000) 582.
[4] L. Sampaio, E.H.C.P. Sinnecker, G.R.C. Cernicchiaro, M. Knobel, M. Vázquez, J. Velázquez, Phys. Rev. B 61 (2000) 8976.
[5] Y. Ishii, M. Sato, J. Magn. Magn. Mater. 82 (1989) 309.
[6] J. Velázquez, C. García, M. Vázquez, A. Hernando, J. Appl. Phys. 85 (1999) 2768.
[7] R. Ferré, K. Ounadjela, J. George, L. Piraux, S. Dubois, Phys. Rev. B 56 (1997) 14066.
[8] C. Seberino, H. Bertram, J. Appl. Phys. 85 (1999) 5543.
[9] D. Hinzke, U. Nowak, J. Magn. Magn. Mater. 221 (2000) 365.
[10] D.R. Fredkin, T.R. Koehler, IEEE Trans. Magn. 26 (1990) 415.
[11] D. Süß, T. Schrefl, J. Fidler, J. Chapman, J. Magn. Magn. Mater. 196–197 (1999) 617.
[12] R. Hertel, H. Kronmüller, Phys. Rev. B 60 (1999) 7366.
[13] T.R. Koehler, D.R. Fredkin, IEEE Trans. Magn. 27 (1991) 4763.
[14] H.-B. Braun, J. Appl. Phys. 85 (1999) 6172.